Since January 2020 Elsevier has created a COVID-19 resource centre with free information in English and Mandarin on the novel coronavirus COVID-19. The COVID-19 resource centre is hosted on Elsevier Connect, the company's public news and information website.

Virus Research 147 (2010) 107–112

Contents lists available at ScienceDirect

Virus Research

journal homepage: www.elsevier.com/locate/virusres

Chemokine profiling of Japanese encephalitis virus-infected mouse neuroblastoma cells by microarray and real-time RT-PCR: Implication in neuropathogenesis

Nimesh Gupta, S.R. Santhosh, J. Pradeep Babu, M.M. Parida, P.V. Lakshmana Rao *

Division of Virology, Defence Research and Development Establishment, Jhansi Road, Gwalior 474002, India

ARTICLE INFO

Article history:
Received 5 August 2009
Received in revised form 23 October 2009
Accepted 24 October 2009
Available online 5 November 2009

Keywords:
Mouse neuroblastoma cells
Japanese encephalitis
Chemokine
Microarray
Gene expression

ABSTRACT

Japanese encephalitis (JE) is one of the leading causes of acute encephalopathy affecting children and adolescents in the tropics. JE virus (JEV) infection causes prominent neurological sequelae in approximately one-third of the survivors. In humans, the inflammatory response of CNS consequent to JEV induced viral encephalitis is mediated through chemokines released by various cells of CNS. In the present study, the chemokine profiles of mouse neuroblastoma cells (N2A) following JEV infection was analyzed by cDNA microarray followed by real-time RT-PCR. Eighty mRNA transcripts belonging to various functional classes exhibited significant alterations in gene expression. There was considerable induction of genes involved in apoptosis and anti-viral response. Modified levels of several transcripts involved in proinflammatory and anti-inflammatory processes exemplified the balance between opposing forces during JEV pathogenesis. Other genes displaying altered transcription included those associated with host translation, cellular metabolism, cell cycle, signal transduction, transcriptional regulation, protein trafficking, neurotransmitters, neuron maturation, protein modulators, ER stress and cytoskeletal proteins. The infection of neurons results in the synthesis of proinflammatory chemokines, which are early important mediators of leukocyte recruitment to sites of viral infection. Our results clearly suggest the implication of chemokines in neuropathogenesis of JEV infection leading to neurological sequelae. Pro- and anti-inflammatory agents targeted against chemokines such as CXCL10 may provide possible therapeutic modalities that can mitigate the morbidity associated with JEV infection of the CNS.

Japanese encephalitis has become a major cause of mortality and morbidity in wide areas of south and southeast Asia and kept in a zoonotic transmission cycle between pigs or birds and mosquitoes (Burke et al., 2001; Solomon et al., 2003; Tsai, 2000). JEV spreads to dead-end hosts, including humans, through the bite of JEV-infected mosquitoes and causes infection of the central nervous system, with a high mortality rate (Parida et al., 2006a). JEV targets the CNS, clinically manifesting with fever, headache, vomiting, signs of meningeal irritation, and altered consciousness, leading to high mortality and neurological sequelae in some of those who survive (Kumar et al., 1990). After entry into the host, JEV generates a rapid inflammatory response, including peripheral neutrophil leucocytosis or infiltration of neutrophils in extraneural tissue. Clinically, the infection of JEV results in increased levels of cytokines such as macrophage-derived chemotactic factor, TNF, and interleukin-8 (IL-8) in the serum and cerebrospinal fluid (Khanna et al., 1991; Ravi et al., 1997; Singh et al., 2000). The increased levels of inflammatory mediators appear to play a protective role or initiate an irreversible immune response leading to cell death. Despite the fact that Japanese encephalitis is a major disease affecting the tropical world, little is known of its pathogenesis due, partly, to the lack of a suitable animal model and the complex cell interactions in infected individuals. JEV tends to cause a neurotrophic infection, attacking neural rather than non-neural tissues in humans. Experimental studies in rats have demonstrated that neuron cells, especially developing neurons are the major target cells for infection. The role that neurons play in the induction of the immune response following CNS viral infection is poorly understood, largely owing to the belief that these cells are immunologically quiescent. In order to understand the nature and consequence at the transcriptional level, we have carried out the microarray analysis of mock-infected and JE virus-infected murine neuroblastoma cells. The microarray data was validated with qRT-PCR experiments and time point analysis was done to demonstrate the induction of chemokine by JEV-infected neurons as an early defense mechanism. We employed mouse neuronal cells (N2A) as a model system because of the permissiveness of these cells to JEV infection (Murali-Krishna et al., 1995; Yang et al., 2004; Lin et al., 2004; Hong-Lin et al., 2002). In

* Corresponding author. Tel.: +91 751 2233495; fax: +91 751 2341148.
E-mail address: pvlrao@rediffmail.com (P.V.L. Rao).

0168-1702/$ – see front matter © 2009 Elsevier B.V. All rights reserved.
doi:10.1016/j.virusres.2009.10.018

Table 1
List of upregulated genes involved in pathogenesis of mouse neuroblastoma cells (N2A) infected with Japanese encephalitis virus.

Accession no.	Gene name	Gene description	Fold change	*p*-Value
NM_021274	Cxcl10	Chemokine (C–X–C motif) ligand 10	7.71	0.019
NM_013653	Ccl5	Chemokine (C–C motif) ligand 5	6.10	0.041
NM_021384	Rsad2	Viral hemorrhagic septicemia virus (VHSV) induced gene 1	5.11	0.049
NM_023386	Rtp4	Receptor transporting protein 4	4.80	0.01
NM_015783	G1p2	Interferon, alpha-inducible protein	4.25	0.008
NM_011909	Usp18	Ubiquitin specific protease 18	4.17	0.011
NM_011854	Oasl2	2′–5′ oligoadenylate synthetase-like 2	4.06	0.025
NM_145211	Oas1a	2′–5′ oligoadenylate synthetase 1A	3.39	0.092
NM_010501	Ifit3	Interferon-induced protein with tetratricopeptide repeats 3	3.38	0.07
NM_145209	Oasl1	2′–5′ oligoadenylate synthetase-like 1	2.85	0.035
NM_007498	Atf3	Activating transcription factor 3	2.71	0.033
NM_019440	Iigp2	Interferon-g induced GTPase	2.51	0.046
XM_488522	Parp14	Poly(ADP-ribose) polymerase family, member 14	2.39	0.004
NM_173368	Chd6	Chromodomain helicase DNA binding protein 6	2.27	0.084
NM_029720	Creld2	Cysteine-rich with EGF-like domains 2	2.22	0.023
NM_022324	Sdf2l1	Stromal cell-derived factor 2-like 1	2.21	0.005
NM_008326	Irgm	Interferon inducible protein 1	2.16	0.001
NM_173743	2310016F22Rik	Hypothetical protein LOC71898	2.15	0.011
NM_010800	Bhlhb8	Muscle, intestine and stomach expression 1	2.12	0.04
NM_008332	Ifit2	Interferon-induced protein with tetratricopeptide repeats 2	2.11	0.011
NM_013760	Dnajb9	DnaJ (Hsp40) homolog, subfamily B, member 9	2.10	3.96E-04
NM_020583	Isg20	Interferon-stimulated protein	2.02	0.031
NM_172715	A230097K15Rik	Hypothetical protein LOC231510	1.95	0.007
NM_007837	Ddit3	DNA-damage inducible transcript 3	1.93	0.004
NM_197986	1110007F12Rik	Hypothetical protein LOC68487	1.90	0.085
NM_019717	Arl6ip2	ADP-ribosylation factor-like 6 interacting protein 2 isoform 1	1.90	0.126
NM_022310	Hspa5	Heat shock 70 kDa protein 5 (glucose-regulated protein)	1.86	0.076
NM_175397	5830484A20Rik	Sp110 nuclear body protein	1.86	0.066
NM_013760	Dnajb9	DnaJ (Hsp40) homolog, subfamily B, member 9	1.81	0.008
NM_008326	Irgm	Interferon inducible protein 1	1.80	0.030
NM_009283	Stat1	Signal transducer and activator of transcription 1	1.79	0.031
NM_008929	Dnajc3	DnaJ (Hsp40) homolog, subfamily C, member 3	1.75	0.040
NM_008654	Myd116	Myeloid differentiation primary response gene 116	1.75	0.088
NM_030150	D11Lgp2e	DNA segment, Chr 11, Lothar Hennighausen 2, expressed	1.75	0.009
NM_012024	Ppp2r5e	Epsilon isoform of regulatory subunit B56, protein phosphatase 2A	1.72	0.097
NM_013642	Dusp1	Dual specificity phosphatase 1	1.71	0.185
NM_008929	Dnajc3	DnaJ (Hsp40) homolog, subfamily C, member 3	1.71	0.106
NM_013760	Dnajb9	DnaJ (Hsp40) homolog, subfamily B, member 9	1.69	0.002
NM_027057	Wdfy1	WD repeat and FYVE domain containing 1	1.64	0.030
NM_011990	Slc7a11	Solute carrier family 7 (cationic amino acid transporter, y+ system), member 11	1.63	0.111
NM_022331	Herpud1	Homocysteine-inducible, endoplasmic reticulum stress-inducible, ubiquitin-like domain member 1	1.62	0.021
NM_018738	Igtp	Interferon gamma induced GTPase	1.60	0.017
NM_013606	Mx2	Myxovirus (influenza virus) resistance 2	1.60	0.002

The microarray data pertains to 36 h post-infection.

this study, we demonstrated that virus infection of neuronal cells results in the strong induction of proinflammatory chemokines along with robust anti-viral response. The replicating virus within the infected host neurons alters normal gene expression profiles, which can be of significance in JEV pathogenesis at the molecular level.

A neurovirulent JEV strain, JE S982, was employed throughout this study. The propagation of virus was carried out in C6/36 cells utilizing RPMI-1640 medium containing 10% fetal bovine serum. To determine virus titers, culture media were harvested for plaque-forming assays using Porcine stable Kidney cells. The mouse neuroblastoma, N2A cell line was maintained in antibiotic-free minimum essential medium (MEM) with Earle's salts supplemented with 2 mM L-glutamine and 10% fetal bovine serum.

For viral infection, monolayers of the mouse neuroblastoma cells grown in 6- or 12-well plates were exposed to either live JE Virus (multiplicity of infection MOI = 5) or mock-infected for 1 h, at 37 °C. The unbound virus was removed from cells by gentle washing with phosphate-buffered saline (PBS), and then the cells were cultured in medium at 37 °C. The quantification of the viral load in harvested infected culture fluid was determined by one-step single tube SYBR Green I mediated JEV Env gene-specific real-time RT-PCR and RT-LAMP (Santhosh et al., 2007; Parida et al., 2006b). Total RNA was extracted from uninfected or JEV-infected cells at 36 h post-infection using the Qiagen (Valencia, CA) RNAEasy Mini kit. RNA quality and integrity was assessed using RNA 6000 Nano Lab Chip on the 2100 Bioanalyzer (Agilent, Palo Alto, CA). Agilent mouse whole genome array (4× 44k; G 4122F) was used and processed for labeling and hybridization as per manufacturer's protocol.

Hybridized arrays were scanned at 5 μm resolution on an Agilent DNA Microarray Scanner, Model G2565BA. Data extraction from images was done using Feature Extraction software of Agilent. The microarray experiment was repeated once. Feature extracted data was analyzed using GeneSpring Gx v7.3.1 software from Agilent. Normalization of the data was done using per spot per chip intensity dependent lowess normalization. Further quality control of normalized data was done using correlation based condition tree to eliminate experimental error. One folds and above differentially regulated genes was filtered from the data. Differentially regulated genes were clustered using gene tree to identify significant gene expression patterns. Ontology based biological analysis was done using Gene Ontology browser in GeneSpring Gx.

Genes with significant transcriptional changes known to be associated with biological significance were selected for further analysis. RT^2 Profiler PCR Array of Mouse Inflammatory Cytokines and Receptors (PAMM-011A Superarray Bioscience Corporation, USA) was used for qRT-PCR studies. The housekeeping genes were used for standardization of the initial RNA content of a sample. The

Table 2
List of downregulated genes involved in pathogenesis of mouse neuroblastoma cells (N2A) infected with Japanese encephalitis virus.

Accession no.	Gene name	Gene description	Fold change	*p*-Value
NM_133743	Lypd3	GPI-anchored metastasis-associated protein homolog	−0.60	0.123
NM_010317	Gng4	Guanine nucleotide binding protein (G protein), gamma 4 subunit	−0.60	0.107
NM_025681	Lix1	Limb expression 1 homolog	−0.60	0.099
XM_001005167	Synpo2		−0.60	0.098
NM_010826	Mrvi1	MRV integration site 1 isoform a	−0.60	0.093
NM_027820	8430429K09Rik	Hypothetical protein LOC71523	−0.60	0.112
	AK080781		−0.60	0.105
NM_144556	Lgi4	Leucine-rich repeat LGI family, member 4	−0.60	0.127
	4933400F03Rik		−0.60	0.153
NM_010585	Itpr1	Inositol 1,4,5-triphosphate receptor 1	−0.60	0.096
XM_622260	AI427138		−0.60	0.149
NM_028133	Egln3	EGL nine homolog 3	−0.60	0.130
NM_028940	4933402J24Rik	Hypothetical protein LOC74438	−0.61	0.095
NM_053139	Pcdhb14	Protocadherin beta 14	−0.61	0.143
NM_138661	Pcdha9	Protocadherin alpha 9	−0.61	0.036
NM_011373	St6galnac4	ST6 (alpha-N-acetyl-neuraminyl-2,3-beta-galactosyl-1,3)-N-acetylgalactosaminide alpha-2,6-sialyltransferase 4	−0.61	0.112
	8430408O14		−0.61	0.102
NM_011867	Slc26a4	Pendrin	−0.61	0.096
XM_125817	1300007O09Rik		−0.61	0.102
NM_133683	Tmem19	Transmembrane protein 19	−0.62	0.096
XM_204152	Frmpd1		−0.62	0.099
NM_001029889	Gm608	Hypothetical protein LOC207806	−0.62	0.108
NM_053146	Pcdhb21	Protocadherin beta 21	−0.62	0.931
NM_008666	Myt1l	Myelin transcription factor 1-like	−0.63	0.088
NM_009824	Cbfa2t3h	Core-binding factor, runt domain, alpha subunit 2, translocated to, 3 homolog	−0.63	0.099
	6330439K17Rik		−0.63	0.095
	Gm288		−0.63	0.156
NM_175383	B3gnt6	Beta-1,3-N-acetylglucosaminyltransferase bGnT-6	−0.63	0.091
NM_009211	Smarcc1	SWI/SNF related, matrix associated, actin dependent regulator of chromatin, subfamily c, member 1	−0.63	0.092
XM_485743	D630002J15Rik		−0.63	0.095
NM_178444	Egfl7	Vascular endothelial statin isoform 1 precursor	−0.63	0.095
NM_030137	Cstad	CSA-conditional, T cell activation-dependent protein	−0.63	0.092
NM_207298	Ceecam1	Cerebral endothelial cell adhesion molecule 1	−0.63	0.109
NM_198119	Lrrc24	Leucine-rich repeat containing 24	−0.64	0.087
	C130057N11Rik		−0.64	0.142
NM_027865	Tmem25	Transmembrane protein 25	−0.64	0.107
NM_025823	Pcyox1	Prenylcysteine oxidase 1	−0.64	0.089
NM_012014	Gprin1	G protein-regulated inducer of neurite outgrowth 1	−0.64	0.089
XM_485800	Aak1		−0.64	0.105
XM_981846	Col22a1		−0.64	0.097
NM_001039079	Prkcz	Protein kinase C, zeta isoform b	−0.64	0.040
NM_025285	Stmn2	Stathmin-like 2	−0.65	0.092
NM_020043	Nope	Neighbor of Punc e11 protein	−0.65	0.106
XM_283153	Polr3g		−0.65	0.101
	C230014O12Rik		−0.65	0.131
XM_130797	Tnik		−0.65	0.103
NM_013884	Cspg5	Chondroitin sulfate proteoglycan 5	−0.65	0.104
NM_172861	Slc7a14	Solute carrier family 7, member 14	−0.65	0.097

The microarray data pertains to 36 h post-infection.

result for an individual sample was expressed as the mean expression level of a specific gene. The relative expression between each infected sample and the uninfected control was then calculated and expressed as fold change.

The real-time RT-PCR was carried out for the time point analysis of chemokines using gene-specific primers for CXCL9, CXCL10, and CXCL11 using Quanti Tect primer assay kit (Qiagen, Germany) and Quanti Fast one-step RT-PCR kit (Qiagen, Germany) to validate the secretion of chemokines by neurons itself as preliminary antiviral response. Reactions were run on Stratagene Mx 3005p system. The threshold cycle (C_t) of gene of interest and housekeeping gene (HK) and the difference between their C_t values (C_t) were determined. Relative changes of gene expression were calculated by the following formula (Livak and Schmittgen, 2001), and the data are represented as fold upregulation/downregulation.fold change = $2^{-\Delta\Delta C_t}$, where $\Delta\Delta C_t$ = (C_t of gene of interest, treated − C_t of HK gene, treated) − (C_t of gene of interest, control − Ct of HK gene, control), C_t is the threshold cycle number and HK is the house keeping gene.

The time point for microarray and PCR array study consisted of only 36 hpi of mock-infected (control) and JE virus-infected samples. For microarray and PCR array, two replicates each (control and infected) were used and the experiment is repeated once. The data of Tables 1–4 were analyzed by *t*-test and *p*-value of ≤0.05

Table 3
Significant pathways of the upregulated genes at 36 h post-infection with JE virus.

Pathways	No. of genes	*p*-Value
Protein export	2	5.46E−06
Toll-like receptor signaling pathway	7	1.88E−05
Circadian rhythm	5	3.22E−05
SNARE interactions in vesicular transport	5	0.000157
MAPK signaling pathway	14	0.0005
Alanine and aspartate metabolism	3	0.002
Aminoacyl-tRNA synthetases	3	0.002
Antigen processing and presentation	4	0.004
One carbon pool by folate	2	0.005
Jak-STAT signaling pathway	5	0.008
Methane metabolism	1	0.023
Novobiocin biosynthesis	1	0.035
N-glycan biosynthesis	2	0.048
Parkinson's disease	2	0.050
Glycosylphosphatidylinositol (GPI)-anchor biosynthesis	1	0.053
Retinol metabolism	1	0.058

Table 4
Significant pathways of the downregulated genes at 36 h post-infection with JE virus.

Pathway	No. of genes	*p*-Value
Biosynthesis of steroids	5	0.0006
Androgen and estrogen metabolism	1	0.013
ECM-receptor interaction	4	0.015
Glycan structures – biosynthesis 2	2	0.019
Diterpenoid biosynthesis	1	0.021
Focal adhesion	6	0.024
Alkaloid biosynthesis I	1	0.031

was considered significant. Data of time course study on chemokine synthesis was analyzed by one-way ANOVA followed Dunnet's test for comparison between control and treatment groups. The level of significance was set at $p \leq 0.05$. All experiments were repeated at least thrice.

Viral replication in N2A cells infected with JE virus JaOAr S982 for 96 h duration was determined by plaque assay of the virus released in the cell culture medium (Fig. 1). The results showed

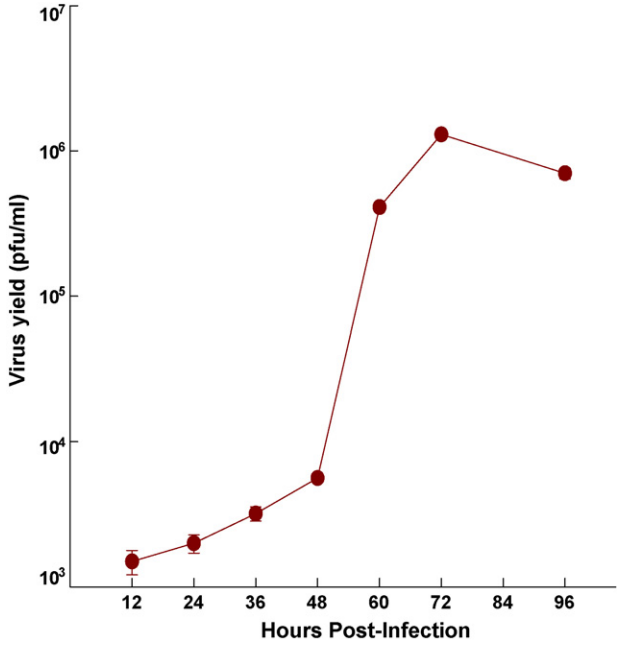

Fig. 1. Kinetics of JEV growth in Mouse N2A cells. Monolayers of N2A cells were infected with the JE S982 strain of JEV at an MOI of ~5 and incubated at 37 °C. At various time intervals, samples were removed and virus titre was assayed. Values are mean ± SE of three replicates each.

that new extracellular viral progeny reached maximum at 72 h. After 72 h, a degree of cell death becomes apparent and the experiment was terminated at 96 h (Fig. 2). Transcript analysis on 36 h post-infection was thus selected to track early changes in gene expression in JE virus-infected cells. A total of 497 genes were found to be significantly upregulated after JEV infection and 223 genes were downregulated (Tables 1 and 2). Some of the pathways which show upregulated gene expression are toll-like receptor signaling, MAPK, JAK-STAT, SNARE reactions in vesicular transport, antigen processing and presentation (Table 3). Some of the significantly downregulated pathways are biosynthesis of steroids, androgen and estrogen metabolism, ECM interaction, focal adhesion, etc. (Table 4). Other downregulated genes are making clusters in CNS signature like neuron maturation, nerve ensheathment, neurophysiological process, transmission of nerve impulse, ionic insulation of neurons, myelination, transport, localization and neuron projection (data not shown). Other differentially regulated genes that were significantly changed include those associated with cell signaling, lipid metabolism, cell cycle and vesicular transport.

In order to verify the reproducibility of the microarray results, the real-time PCR plate assay of mouse inflammatory cytokines and cytokine receptors was carried out. The results showed a set of six genes viz. Itgb, CD40, Tollip, Xcr1, CXCL1 and CXCL10 well corroborated with microarray data. GAPDH, β actin, Gusb, Hsp90 ab1 and Hprt1 were used as housekeeping genes. Out of those six genes, five genes showed congruent and significant differences in expression, while one displayed opposite expression pattern (Table 5). Upregulated genes include CXCL1 (chemokine, C–X–C motif, ligand 1), CXCL10 (chemokine, C–X–C motif, ligand 10), Itgb (integrin beta), and CD 40 (CD40 ligand). downregulated genes include Xcr1 (chemokine, C motif receptor 1). However, the qRT-PCR showed greater dynamism in fold changes than the microarray results because of the greater sensitivity of PCR compared with fluorescent detection in microarray experiment.

We found marked increase in expression of IP-10/CXCL10, which is known to play important role in the host defense against viral infection (Chen et al., 2006). CXCL10 is found to be a crucial molecule governing the protective response against various diseases like dengue, *Trypanosoma cruzi*, *Klebsiella pneumoniae*, rabies virus and corona virus infection of the CNS by enhancing innate immune responses (Hsieh et al., 2006; Hardison et al., 2006). IP-10 is an essential component in host defense by coordinating the trafficking of Th1 T lymphocytes into the CNS in response to viral infection. We demonstrated the strong induction of CXCL10 by infected neurons itself. The qRT-PCR analysis showed sustained induction of CXCL10 in JEV-infected mouse neuroblastoma cells. The results indicate that neurons may be a source of chemokine

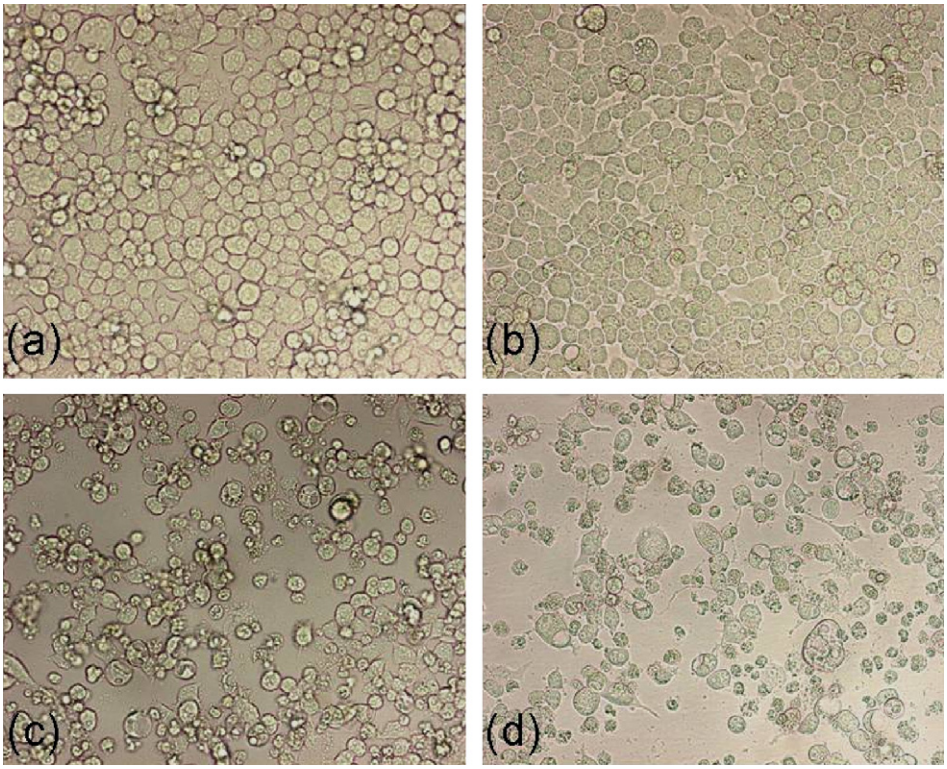

Fig. 2. Morphological pattern of neuroblastoma cells infected with JEV. Monolayers of the mouse neuroblastoma cells were adsorbed with either live JE virus (multiplicity of infection (MOI) ~5) or mock-infected for 1 h, at 37 °C. (a) N2A cells mock-infected at 36 hpi; (b) N2A cells infected with JEV at 36 hpi; (c) N2A cells infected with JEV at 72 hpi; (d) N2A cells infected with JEV at 96 hpi.

synthesis for primary anti-viral response in JE infection (Fig. 3B). There is gradual decrease in CXCL10 expression with increased viral load in cells, suggesting its anti-viral role in JE infection. No significant fold change was detected for other chemoattractant like CXCL11 and CXCL9 (Fig. 3A–C).

Array data also showed Ccl-5 upregulation in JE infection indicating virus modulation of the host machinery in the initial stages of infection. Ccl5–Ccr5 interaction provides anti-apoptotic signals for macrophage survival during viral infection. Ccl5-responsive genes comprise a significant number of enzymes, transcription factors, and miscellaneous molecules involved in neuronal survival and differentiation, including neurite outgrowth and synaptogenesis (Valerio et al., 2004). There was significant upregulation of a number of ubiquitin–proteasome system related genes such as Usp18 during JE virus replication but it was unclear if this response was anti-viral or if the JE virus utilized components of the ubiquitin–proteasome system for its replication. We found significant upregulation in anti-viral response genes like IFN induced Isg15, Viperin, Mx 2, anti-viral genes like oligoadenylate synthetase, Parp14, Irgm, transcription factor-like STAT and ER stress regulated genes like Herpud1, ATF6 and XBP1. The marked elevation in expression of these genes at 36 h post-infection suggests a highly notable anti-viral response to JEV pathogenesis.

Downregulated genes were mainly from focal adhesion and CNS signature, as detailed and vast study is required to elaborate the importance and involvement of these significantly downregulated genes in JEV pathogenesis. Genes like Lypd3, Lgi4 are involved in protein binding, neuron maturation, myelination, etc. The real-time RT-PCR validated genes elucidate the varied transcriptional responses of JE virus-infected neuroblastoma cells. Together with other identified differentially expressed genes, these transcripts provide a better understanding of the pathogenesis of JEV at a transcriptomic level, particularly the molecular events that underpin host defense mechanism against JEV infection.

The results of the present study with mouse neuronal cells clearly show that many genes and host response pathways were upregulated during JE infection. Specific components of the response to virus such as Viperin, G1p2, Ifit3, Atf3, Irgm and CXCL10 have been implicated in JE infection for the first time to the best of our knowledge. Future research is required to explore the mechanism of JEV modulation of these genes to evade the host defense response. Our study offers an overview of the cascade of changes in host cellular expression culminating from infection with JEV. The counterbalancing of several anti-inflammatory and proinflammatory pathways together with the variable expression of apoptosis-related genes is a significant finding of the present study. The involvement of these genes indicated modulation of ini-

Table 5
Comparison of gene expression changes between microarray and qRT-PCR of some select genes in mouse neuroblastoma cells at 36 h post-infection with JE virus.

Gene name	Description	Pathway	Microarray	Real-time RT-PCR
Itgb	Integrin beta	Focal adhesion, ECM-receptor interaction	+1	+1.42
CD40	CD40 ligand	Toll-like receptor signaling	+1.06	+1.6
Tollip	Toll interacting protein	Toll-like receptor signaling	−0.61	+1.40
Xcr1	Chemokine (C motif) receptor 1	Cytokine–cytokine receptor interaction	−0.3	−0.5
Cxcl1	Chemokine (C–X–C motif) ligand 1	Cytokine–cytokine receptor interaction	+3.1	+6.68
Cxcl10	Chemokine (C–X–C motif) ligand 10	Toll-Like receptor signaling	+7.7	+35.7

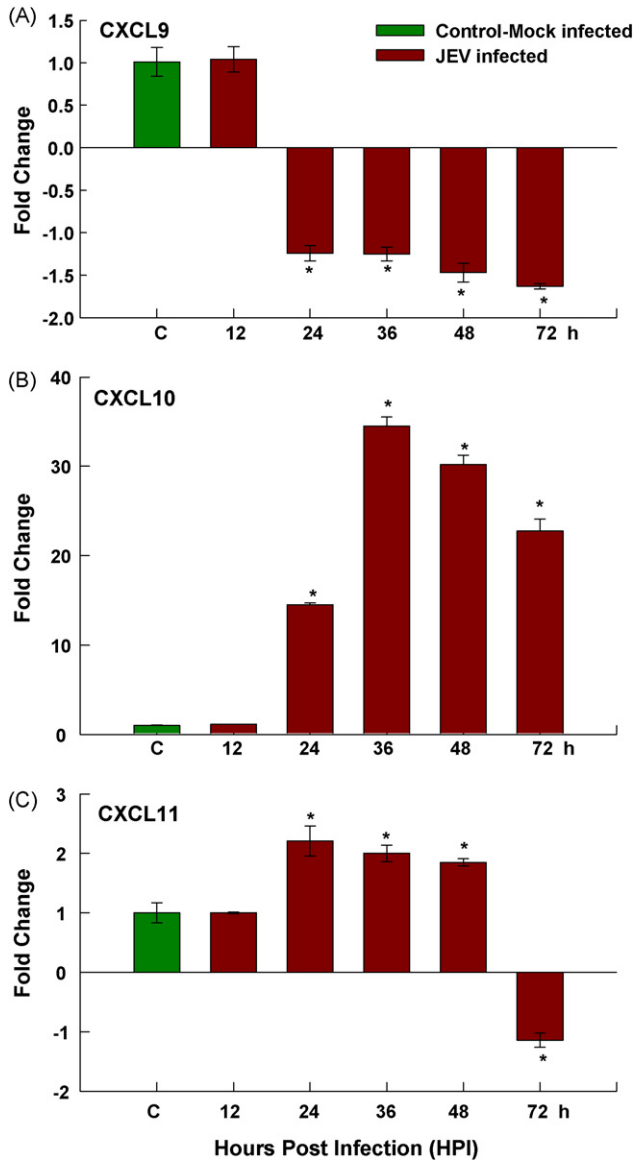

Fig. 3. Chemokine expression by JEV-infected mouse neuroblastoma. N2A cells were infected with JEV, at least three replicates per time point were collected at different time intervals, and analysis was done with real-time RT-PCR. The expression of (A) CXCL9, (B) CXCL10 and (C) CXCL11 are shown. Values are mean ± SE of three replicates each. *Significantly different from control at $p < 0.05$ by Dunnet's test.

tial host cell response and balance between cell proliferation and cell death there by enabling virus multiplication. The emerging picture from this study implicates a central role for the immune response in the pathobiology of JE infection. It will be interesting to compare the host response to different JEV isolates with inactivated preparations of the virus.

The present study implies that neurons play an important role in their own defense against viral infections. Although this challenges the long-held belief that neurons are immunologically quiescent, an improved understanding of the proinflammatory effects responsible for immune-mediated control of viral infection and neuronal injury during JEV infection is an essential step for developing strategies for limiting the severity of CNS disease.

Acknowledgements

We thank Dr. R. Vijayaraghavan, Director, DRDE for offering all facilities and support required for this study. Mr. Nimesh Gupta is recipient of DRDO Senior research fellowship.

References

Burke, D.S., Monath, T.P., Flaviviruses,., Knipe, D.M., Howley, P.M., Griffin, D.E., Lamb, R.A., Martin, M.A., Roizman, B., Straus, S.E. (Eds.), 2001. Fields Virology, vol. 1, 4th ed. Lippincott Williams & Wilkins, Philadelphia, pp. 1043–1125.

Chen, J.P., Lu, H.L., Lai, S.L., Campanella, G.S., Sung, J.M., Lu, M.Y., Wu-Hsieh, B.A., Lin, Y.L., Lane, T.E., Luster, A.D., Liao, F., 2006. Dengue virus induces expression of CXC chemokine ligand 10/IFN-gamma-inducible protein 10, which competitively inhibits viral binding to cell surface heparan sulfate. J. Immunol. 177, 3185–3192.

Hardison, J.L., Wrightsman, R.A., Carpenter, P.M., Lane, T.E., Manning, J.E., 2006. The chemokines CXCL9 and CXCL10 promote a protective immune response but do not contribute to cardiac inflammation following infection with *Trypanosoma cruzi*. Infect. Immun. 74, 125–134.

Hong-Lin, Su, Ching-Len, Liao, Lin, Yi-Ling, 2002. Japanese encephalitis virus infection initiates endoplasmic reticulum stress and an unfolded protein response. J. Virol., 4162–4171.

Hsieh, M.F., Lai, S.L., Chen, J.P., Sung, J.M., Lin, Y.L., Wu-Hsieh, B.A., Gerard, C., Luster, A., Liao, F., 2006. Both CXCR3 and CXCL10/IFN-inducible protein 10 are required for resistance to primary infection by dengue virus. J. Immunol. 177, 1855–1863.

Khanna, N., Agnihotri, M., Mathur, A., Chaturvedi, U.C., 1991. Neutrophil chemotactic factor produced by Japanese encephalitis virus stimulated macrophages. Clin. Exp. Immunol. 86, 299–303.

Kumar, R., Mathur, A., Kumar, A., Sethi, G.D., Sharma, S., Chaturvedi, U.C., 1990. Virological investigations of acute encephalopathy in India. Arch. Dis. Child. 65, 1227–1230.

Lin, R.J., Liao, C.L., Lin, Y.L., 2004. Replication-incompetent virions of Japanese encephalitis virus trigger neuronal cell death by oxidative stress in a culture system. J. Gen. Virol. 85, 521–533.

Livak, K.J., Schmittgen, T.D., 2001. Analysis of relative gene expression data using real- time quantitative PCR and the $2^{-\Delta\Delta CT}$ method. Methods 25, 402–408.

Murali-Krishna, K., Ravi, V., Manjunath, R., 1995. Japanese encephalitis virus infection of mouse cell lines: ability to prime mice for generation of virus specific cytotoxic T lymphocytes and differences in CTL recognisable viral determinants. Arch. Virol. 140, 127–143.

Parida, M.M., Dash, P.K., Tripathi, N.K., Ambuj, Santhosh, S.R., Saxena, P.S., Agarwal, S., Sahni, A.K., Singh, S.P., Rathi, A.K., Bhargava, R., Abhyankar, A., Verma, S.K., Rao, P.V.L., Sekhar, K., 2006a. Japanese encephalitis outbreak, India, 2005. Emerg. Infect. Dis. 12, 1427–1430.

Parida, M.M., Santhosh, S.R., Dash, P.K., Tripathi, N.K., Saxena, P., Ambuj, Sahni, A.K., Rao, P.V.L., Morita, K., 2006b. Development and evaluation of reverse transcription Loop mediated isothermal amplification assay for rapid and real-time detection of Japanese encephalitis virus. J. Clin. Microbiol. 44 (11), 4172–4178.

Ravi, V., Parida, S., Desai, A., Chandramuki, A., Gourie-Devi, M., Grau, G.E., 1997. Correlation of tumor necrosis factor levels in the serum and cerebrospinal fluid with clinical outcome in Japanese encephalitis patients. J. Med. Virol. 51, 132–136.

Santhosh, S.R., Parida, M.M., Dash, P.K., Pateriya, A., Pattnaik, B., Pradhan, H.K., Tripathi, N.K., Ambuj, S., Gupta, N., Saxena, P., Rao, P.V.L., 2007. Development and evaluation of SYBR Green I-based one-step real time RT-PCR assay for detection and quantification of Japanese encephalitis virus. J. Virol Methods 143, 73–80.

Singh, A., Kulshreshtha, R., Mathur, A., 2000. Secretion of the chemokine interleukin-8 during Japanese encephalitis virus infection. J. Med. Microbiol. 49, 607–612.

Solomon, T., Ni, H., Beasley, D.W., Ekkelenkamp, M., Cardosa, M.J., Barrett, A.D., 2003. Origin and evolution of Japanese encephalitis virus in southeast Asia. J. Virol. 77, 3091–3098.

Tsai, T.F., 2000. New initiatives for the control of Japanese encephalitis by vaccination: minutes of a WHO/CVI meeting, Bangkok, Thailand. Vaccine 26, 1–25.

Valerio, A., Ferrario, M., Martinez, F., Locati, O.M., Ghisi, V., Bresciani, L.G., Mantovani, A., Spano, A.P., 2004. Gene expression profile activated by the chemokine CCL5/RANTES in human neuronal cells. J. Neurosci. Res. 78, 371–382.

Yang, K.D., Yeh, W.T., Chen, R.F., Chuon, H.L., Tsai, H.P., Yao, C.W., Shaio, M.F., 2004. A model to study neurotropism and persistency of Japanese encephalitis virus infection in human neuroblastoma cells and leukocytes. J. Gen. Virol. 85, 635–642.